J Mater Sci: Mater Electron (2017) 28:9295–9300
DOI 10.1007/s10854-017-6666-3

Optimization of the annealing process and nanoscale piezoelectric properties of (002) AlN thin films

Bangran Fu[1] · Fang Wang[1] · Rongrong Cao[1] · Yemei Han[1] · Yinping Miao[1] · Yulin Feng[1] · Fuliang Xiao[1] · Kailiang Zhang[1]

Received: 7 November 2016 / Accepted: 26 February 2017 / Published online: 13 March 2017

Abstract In this paper, the effects of different annealing processes on the texture, surface morphology, and piezoelectric properties of aluminum nitride (AlN) thin films and the performance of AlN-based surface acoustic wave (SAW) devices were systematically investigated. Based on the crystallinity and the morphology results, it is evident that in-situ annealing method is superior to ex-situ annealing. For the AlN thin films, the crystallization and piezoelectricity were both enhanced and then receded as the annealing temperature increased from 300 to 600 °C. We demonstrated that good (002) orientation, excellent grain distribution and high relative piezoelectric coefficient of the AlN thin films were achieved via in-situ annealing at 500 °C. Meanwhile, the AlN thin films exhibited excellent polarization properties and polarization maintaining characteristics. Additionally, the uniform interdigital transducer (IDT) with 8 μm period (finger width = 2 μm) were designed and the IDT/AlN/SiO_2/Si SAW devices with the center frequency f_0 of 495 MHz and insert loss of −24.1 dB were fabricated.

1 Introduction

Aluminum nitride (AlN) is an III-V piezoelectric material with wide bandgap, outstanding hardness, and high electrical resistivity. Thus, it has been widely applied in surface acoustic wave (SAW) devices and pressure sensors [1]. Specifically, *c*-axis AlN thin films have attracted great interest as piezoelectric materials because of their high acoustic velocity (9650 m/s and 5500 m/s for longitudinal and transversal bulk waves, respectively, and 5607 m/s for Rayleigh wave). Moreover, *c*-axis AlN thin films also maintain a high piezoelectric coupling factor, strong electromechanical coupling coefficient of 0.3%, and remarkable chemical and thermal stability [2–4]. Therefore, AlN thin films with high *c*-axis orientation are expected as the promising candidate for SAW devices.

Recently, several deposition techniques have been applied to prepare high *c*-axis textured AlN thin films on different substrates, including molecular beam epitaxial, metal–organic chemical-vapor deposition, pulsed laser deposition, and magnetron sputtering [5]. However, previous experimental studies focused on the sputtering parameters, such as pressure, power, sputtering ambient and target-substrate distance [6, 7]. Regarding the sputtering method, the high substrate temperature is essential. However, the prepared AlN thin films often have a low crystallinity and large residual stress [8]. Recently, it is reported that annealing could improve the crystallization of the films [9]. However, very few researches studied the influence of the post-annealing treatment on the surface morphology, crystallization orientation, or piezoelectric coefficient of AlN thin films.

In this work, effects of different annealing conditions on the surface morphology, crystallinity, and piezoelectric coefficient of AlN thin films were investigated. The thin films were directly deposited on SiO_2/Si and Pt/Ti/SiO_2/Si substrates using direct current (DC) magnetron sputtering, and then they were annealed in N_2 atmosphere for 30 min at temperatures ranging from 300 to

✉ Fang Wang
fwang75@163.com

✉ Kailiang Zhang
kailiang_zhang@163.com

[1] School of Electrical and Electronic Engineering, Tianjin Key Laboratory of Film Electronic & Communication Devices, Tianjin University of Technology, 391 West Binshui Road, Tianjin 300384, China

600 °C (with an interval of 100 °C) by in-situ and ex-situ method. We investigated the piezoelectricity and polarization characteristics of AlN thin films annealed in-situ at 500 °C. Finally, the SAW devices with 8 μm period (a = 2 μm) interdigital electrodes were fabricated using photolithography, based on the IDT/AlN/SiO_2/Si structure.

2 Experimental

The AlN thin films were deposited using the aluminum target (purity > 99.99%) with a diameter of 60 mm at a pressure of 0.2 Pa. The N_2 gas ratio was 50% in the gas mixture and the target-substrate distance was 4.5 cm. The process power was 144 W at room temperature. The samples were annealed under different conditions in N_2 atmosphere for 30 min. The in-situ method was used for heating the substrate to relevant temperatures of 300, 400, 500, 600 °C after deposition. And the ex-situ method was annealed the samples in N_2 atmosphere for 30 min at corresponding temperatures (300, 400, 500, 600 °C) using rapid annealing equipment (RTP-500, Beijing Eastar Labs).

The microstructure of the AlN films was investigated by X-ray diffraction (XRD, Rigaku Ultima IV that using Cu-Kα radiation). The surface morphology and the relative piezoelectric coefficient (d_{33}) of the AlN films were measured using the piezoresponse force microscopy (PFM) system (Agilent 5500). During the PFM measurement, the DC bias voltage was −10 V and the applied alternating current (AC) voltage was from −10 V to +10 V, and then it was switched back to −10 V. The frequency responses of the SAW devices were measured using a network analyzer (Keysight N5232A).

3 Results and discussion

3.1 XRD and AFM analysis

3.1.1 Ex-situ annealing

To improve the crystallographic orientation of (002) aluminum nitride (AlN) thin films, annealing was performed to provide temperature compensation to the recrystallization of the material. To determine the effect of different annealing conditions on the microstructure of the AlN thin films, the XRD patterns of the samples annealed ex-situ at different temperatures are shown in Fig. 1a. The as-deposited AlN thin films were non-crystalline. When the annealing temperature is 300 and 400 °C, the films exhibited orientations of (100) and (101) at 2θ angles of 32.92° and 38.12°, respectively, and they began to show a sharp (002) orientation at 35.98° as the temperature increases to 500 °C. With a further increase in temperature to 600 °C, the (002) orientation faded away. The film surface energy tends to become lower by changing the texture, which leads to the formation of (002) orientation since it exhibits the lowest surface energy ascribed to the closely packed structure. When the temperature is below 500 °C, there is insufficient energy to form (002) orientation films, and only (100) and (101) orientations are formed, which require lower energy [10]. Further increase in temperature up to 500 °C enhanced the mobility of the adatom, which enabled the (002) orientation to be formed. At 600 °C, the reduction of the (002) intensity might be attributed to the formation of lattice defects.

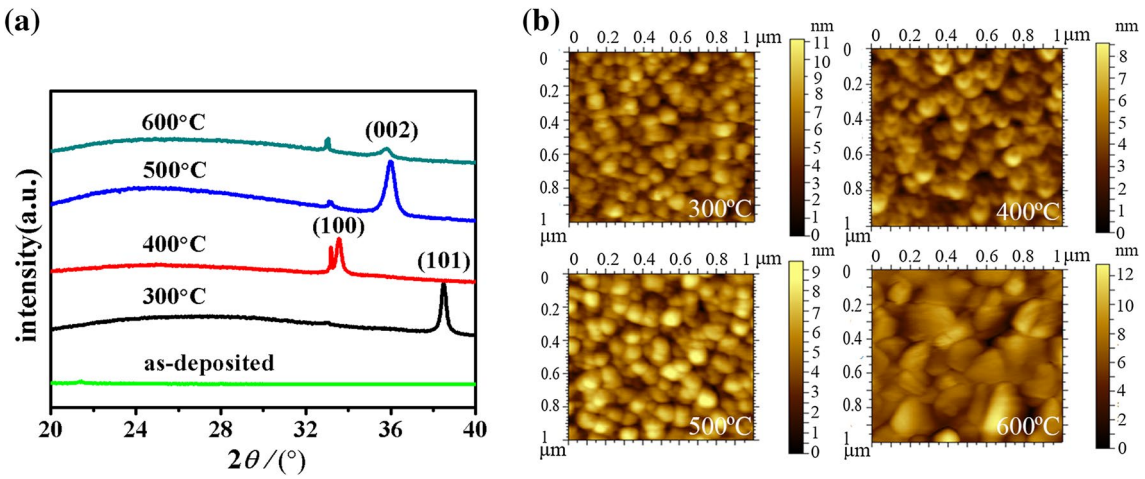

Fig. 1 **a** XRD diffraction pattern and **b** AFM images of the ex-situ annealed AlN films

The surface morphologies of samples were examined, as shown in Fig. 1b. The root mean square (RMS) roughness of these thin films are all in the range of 1–10 nm. As the temperature increasing, the shape and size of the crystal grains change correspondly. At a lower temperature, the grains are preferentially diffused horizontally, giving rise to the formation of (100) and (101) orientation. After obtaining a higher energy, the grains further expand and squeeze each other, making a round grain-like package. Upon further increase in the temperature, the crystal grain size might be too large, resulting in the presence of lattice defects and making lower film crystallinity.

3.1.2 In-situ annealing

The in-situ annealed AlN films exhibited a different tendency, as shown in Fig. 2a. At 300 °C, there was sufficient energy to form the (002) orientation, possibly because it required time to move the adatoms to the lattice site in the (002) orientation at the end of the film deposition. During this period, formation of the (002) orientation may require a lower temperature than the samples annealed using ex-situ method. Moreover, as the temperature increased from 300 to 500 °C, the mobility of the adatoms was enhanced so that the (002) orientation had a higher intensity in the XRD pattern. Additionally, when the temperature was increased to 600 °C, the intensity of the (002) plane began to decrease due to the formation of defects [11].

From the AFM images (Fig. 2b), it is evident that the AlN thin films that were annealed in situ had a better conformance. The XRD analysis results indicate that the films annealed at 500 °C have the best (002) orientation. Moreover, there was a similar trend for the AlN grain size for the two annealing method. As the temperature increased, the grains became better initially and worse in the end. The grains continuously diffused and squeezed into a round bag shape. Additionally, the grain nucleation points were denser, showing a basic trend of vertical diffusion. Meanwhile, due to the slower heating rate, the grains had enough time to diffuse to the region with relatively low surface energy [12]. Therefore, the in-situ annealed samples were better in terms of uniformity and crystallinity.

3.2 PFM and polarization properties analysis

AlN thin films with better microstructure and surface morphology usually exhibit a higher relative piezoelectric coefficient (d_{33}).

$$d_{33} = (A_1 - A_0)/(V_1 - V_0) \quad (1)$$

The d_{33} value can be calculated using Eq. (1), in which A_1 and V_1 correspond to the amplitude and voltage, respectively, of a random point on the butterfly curve, and (A_0, V_0) is the intersection of the butterfly curve. The method for characterizing the piezoelectric properties of the films has been proposed by previous report [13, 14]. The d_{33} value is a relative piezoelectric coefficient, because it is converted to a voltage in the PFM system, but it also indicates a change of the annealed thin films under different conditions. Figure 3 a, b show the butterfly curve and d_{33} curve of the in-situ annealed AlN thin films under different temperatures. As the temperature rises, the maximum values of the amplitude are (a) 4.83 V, (b) 5.98 V, (c) 6.52 V, and (d) 5.23 V. Additionally, the maximum values of the d_{33} are (a) 0.39 V, (b) 0.40 V, (c) 0.52 V, and (d) 0.43 V. The piezoelectric properties exhibit a similar trend as in the XRD analysis. The samples annealed at 500 °C exhibited the optimal piezoelectric properties.

According to the above investigations, the characteristics of the thin films annealed in-situ method for 30 min at 500 °C in N_2 atmosphere were further studied. To study the polarization properties of the AlN thin films, a

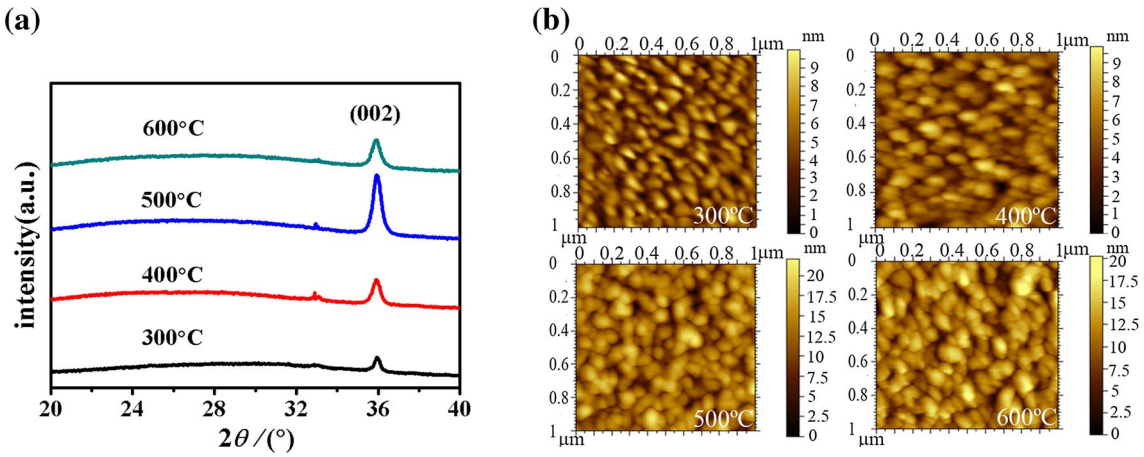

Fig. 2 **a** XRD diffraction pattern and **b** AFM images of the in-situ annealed AlN films

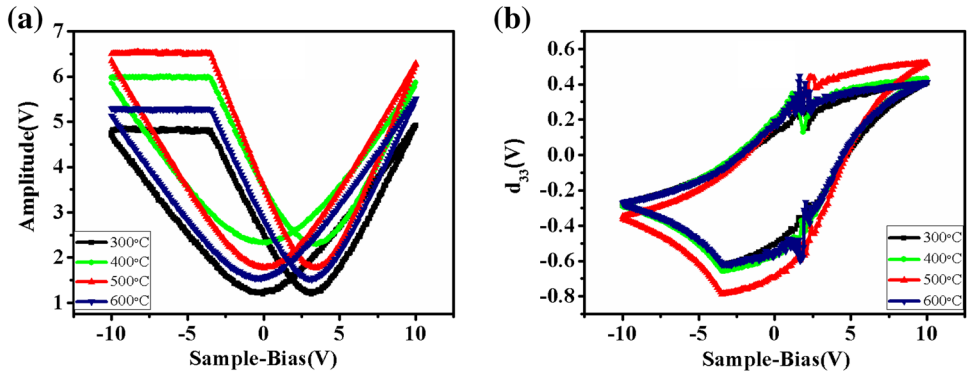

Fig. 3 **a** Butterfly curves and **b** d_{33} curves for the in-situ annealed AlN films at different temperatures

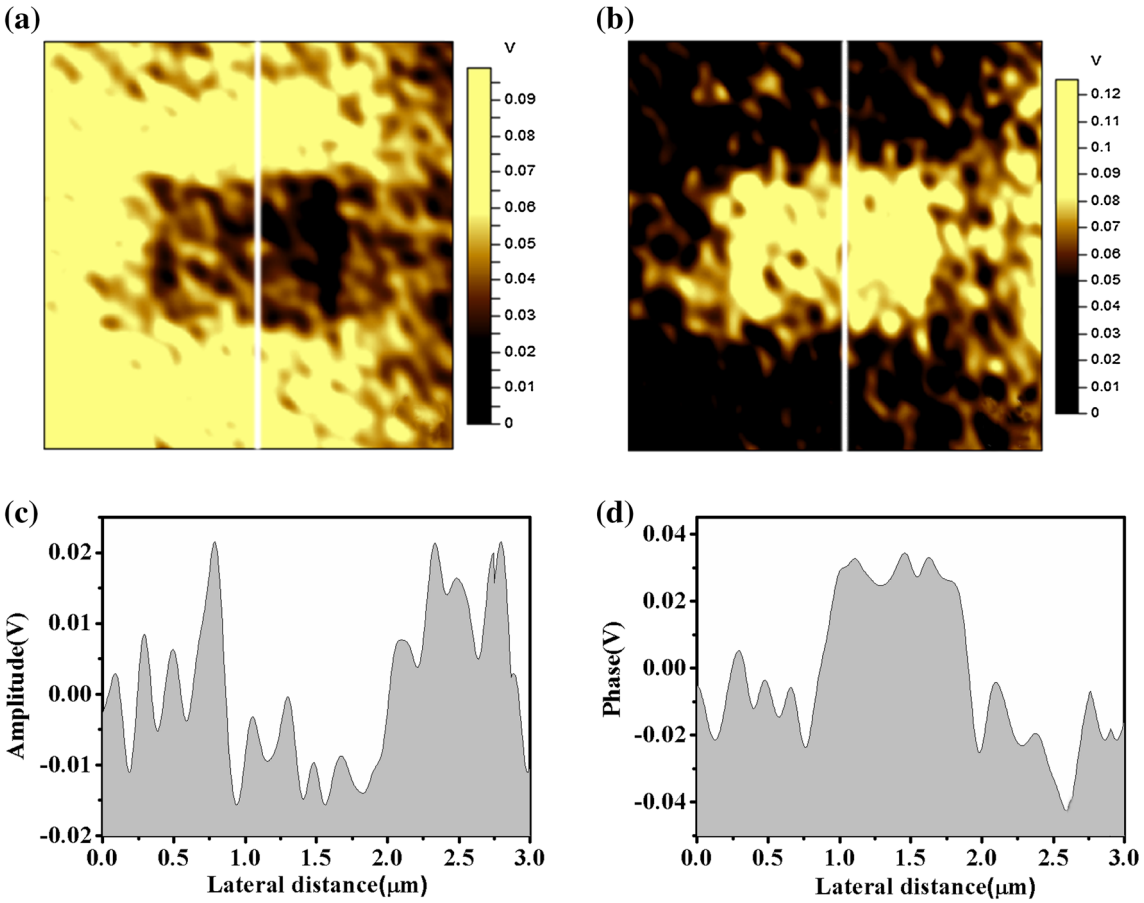

Fig. 4 Polarization of the AlN thin films with different voltages which annealed in-situ method for 30 min at 500 °C in N_2 atmosphere: **a** polarizing amplitude, **b** polarizing phase, **c** cross section cut of the amplitude map, **d** cross section cut of the phase map

1 μm × 1 μm region was first polarized with a voltage of −8 V and then polarized with a voltage of +8 V in the region of 3 μm × 3 μm with the same central core. The amplitude image and phase image are shown in Fig. 4a, b, respectively. The amplitude and phase images of the films exhibited complementary characteristics of expansion and contraction. In the amplitude image, the color of the region that using −8 V polarization is more gloom, indicating that the grains exhibited local contraction. The remaining region was brighter, indicating local expansion for the grains. Additionally, the phase image was contrary to the amplitude image [15, 16]. It shows that the polarization of the AlN film is well polarized with a voltage of −8 V in the region of 1 μm × 1 μm. The grains showed the tendency of local contraction. When +8 V was applied in the region of 3 μm × 3 μm, it had some influences on the polarization

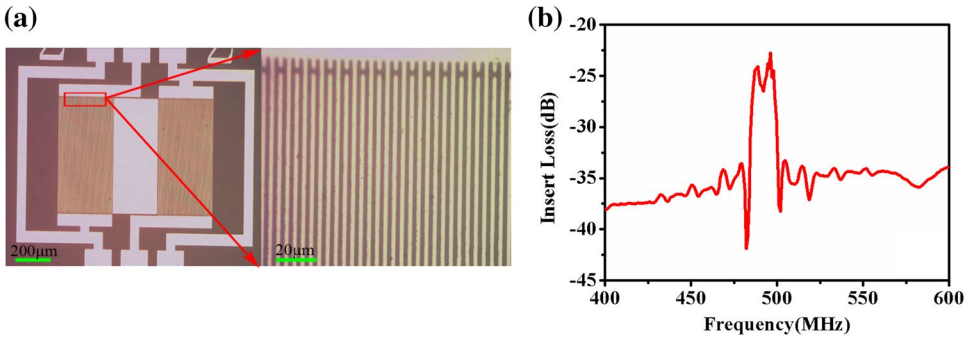

Fig. 5 **a** Structure and **b** frequency responses (S_{21}) of the SAW devices on the AlN thin films that were annealed at 500 °C in situ

region of −8 V, but the polarization direction of the films was basically maintained. Thus, the AlN thin films had good polarization maintaining properties [17]. This is of great significance for the further preparation of SAW devices. To intuitively observe the polarization characteristics of the films, Fig. 4c, d show the cross sectional profiles of the amplitude and phase images that correspond to the white lines in Fig. 4a, b, respectively. Figure 4 c, d clearly show that the polarization direction of the 1 μm × 1 μm region polarized with −8 V is significantly different from the surrounding 3 μm × 3 μm region. The excellent polarization maintaining demonstrates that the (002) AlN thin films exhibit a favorable read and write performance.

3.3 SAW devices fabrication and results

Based on the XRD and PFM analysis, the AlN thin films annealed in situ at 500 °C exhibited the best performance. Thus, SAW devices were fabricated on the AlN thin films annealed under this condition. The thickness of AlN thin films is about 800 nm. In addition, the structure of IDT was obtained using ultra violet lithography. The design parameters for the SAW filter with a metallization ratio of 0.5 are a wavelength of $\lambda = 8$ μm, $N_p = 30$ (IDT finger pairs), $W = 50\lambda$ (acoustic aperture) and $M = 25\lambda$ (delay distance).In order to suppress the false response, IDTs are designed with dummy finger of 4 μm. The metal between the IDTs is 6 μm away from the busbar and the distance between metal and IDT is 2 μm. The images of the IDT are shown in Fig. 5a. Split uniform transducer IDT consists of split-finger electrodes with a finger width of 2 μm. The frequency response characteristics (S_{21}) of the SAW devices are shown in Fig. 5b. When the temperature was 500 °C, the center frequency was up to 495 MHz with a low insert loss of −24.1 dB. This can be explained by the optimization of the crystalline degree of the (002) orientation. When the (002) orientation of AlN thin films becoming better, the films possess a faster acoustic velocity and a higher relative piezoelectric coefficient. Meanwhile, AlN thin films exhibit a larger electromechanical coupling coefficient and energy conversion efficiency, resulting in a lower energy loss. In addition, the energy loss could be also reduced by improving the surface smoothness of AlN thin films.

4 Conclusions

The annealing influences on AlN thin films were investigated. Compared with the ex-situ method, the in-situ annealing method has significant advantages. An annealing temperature of 500 °C was found to be optimal for obtaining (002) orientation of AlN thin films. When the crystallinity of (002) orientation was improved, the relative piezoelectric coefficient was enhanced correspondingly. The crystallization and piezoelectricity were enhanced and then receded with the increase in the annealing temperature from 300 to 600 °C. The polarization direction was basically maintained when the opposite voltage of +8 V was applied to polarized AlN thin films. Thus, it is believed that the AlN thin films annealed in situ at 500 °C have good polarization properties and polarization maintaining characteristics. The relative piezoelectric coefficient d_{33} was 0.52 V, which was higher than the others. Moreover, the finger width of the uniform IDT was designed as 2 μm and SAW devices were fabricated on the structure of IDT/AlN/SiO_2/Si. The excellent piezoelectric properties of AlN thin films that annealed in situ at 500 °C promoted the center frequency of the devices up to 495 MHz. The insert loss of SAW devices was only −24.1 dB due to the flat surface and high d_{33} of the AlN thin films.

Acknowledgements This work is supported by the National Natural Science Foundation of China (Grant Nos. 61404091, 61505144, 51502203, and 51502204) and National Science and Technology Major Project of the Ministry of Science and Technology of China (Grant Nos. 2016YFB0402703) and Tianjin Natural Science Foundation (Grant Nos. 14JCZDJC31500 and 14JCQNJC00800) and Tianjin Science and Technology developmental Funds of Universities and Colleges (Grant Nos. 20130701 and 20130702).

References

1. M. Gillinger, K. Shaposhnikov, T. Knobloch, M. Schneider, M. Kaltenbacher, U. Schmid, Appl. Phys. Lett. **108**, 231601-1-231601-4 (2016)
2. S. Khan, M. Shahid, A. Mahmood, A. Shah, I. Ahmed, M. Mehmooda, U. Azizd, Q. Razad, M. Alamc, Prog. Nat. Sci. **25**, 282–290 (2015)
3. N. Afzal, M. Devarajan, K. Ibrahim, J. Mater. Sci. **27**, 4281–4289 (2016)
4. G.E. Stan, M. Botea, G.A. Boni, I. Pintilie, L. Pintilie, Appl. Surf. Sci. **353**, 1195–1202 (2015)
5. T. Aubert, M.B. Assouar, O. Legrani, O. Elmazria, C. Tiusan, S. Robert, J. Vac. Sci. Technol. A. **29**, 021010-1-021010-6 (2011)
6. H.Y. Liu, G.S. Tang, F. Zeng, F. Pan,J. Cryst. Growth **363**, 80–85 (2013)
7. S.D. Ekpe, F.J. Jimenze, S.K. Dew, J. Vac. Sci. Technol. A **28**, 1210–1214 (2010)
8. A. Pandey, S. Dutta, R. Prakash, S. Dalal, R. Raman, A.K. Kapoor, D. Kaur, Mat. Sci. Semicon. Proc. **52**, 16–23 (2016)
9. V. Kumar, V. Kumar, S. Som, A. Yousif, N. Singh, O.M. Ntwaeaborwa, A. Kapoor, H.C. Swart. J. Colloid Interf. Sci. **428**, 8–15 (2014)
10. S. Benramache, B. Benhaoua, Superlattice Microst. **52**, 1062–1070 (2012)
11. K.-H. Chiu, J.-H. Chen, H.-R. Chen, R.-S. Huang, Thin Solid Films **515**, 4819–4825 (2007)
12. X. Jiao, Y. Shi, H. Zhong, R. Zhang, J. Yang, J. Mater. Sci. **26**, 801–808 (2015)
13. X. Bi, Y. Wu, J. Wu, H. Li, L. Zhou, J. Mater. Sci. **25**, 2435–2442 (2014)
14. Y.C. Yang, C. Song, X.H. Wang, F. Zeng, F. Pan, Appl. Phys. Lett. **92**, 012907 (2008)
15. D. Martin, J. Müller, T. Schenk, T.M. Arruda, A. Kumar, E. Strelcov, E. Yurchuk, M. Stefan, D. Pohl, S. Uwe, S.V. Kalinin, T. Mikolajick, Adv. Mater. **26**, 8198–8202 (2014)
16. Žukauskaitė Agnė, Broitman Esteban, Sandström Per, Lars Hultman, Jens Birch, Phys. Status Solidi A **212**, 666–673 (2015)
17. F. Wang, B. Yang, J. Wei, K. Zhang, IEEE Trans. Nanotechnol. 13, 442–445 (2014)